online data

Cyclic nucleotide phosphodiesterases in *Drosophila melanogaster*

Jonathan P. DAY*, Julian A. T. DOW*, Miles D. HOUSLAY† and Shireen-A. DAVIES*[1]

*Division of Molecular Genetics, Institute of Biomedical and Life Sciences, University of Glasgow, Glasgow G11 6NU, U.K., and †Division of Biochemistry and Molecular Biology, Institute of Biomedical and Life Sciences, University of Glasgow, Glasgow G11 6NU, U.K.

Cyclic nucleotide PDEs (phosphodiesterases) are important enzymes that regulate intracellular levels of cAMP and cGMP. In the present study, we identify and characterize novel PDEs in the genetic model, *Drosophila melanogaster*. The *Drosophila* genome encodes five novel PDE genes in addition to *dunce*. Predicted PDE sequences of *Drosophila* show highly conserved critical domains when compared with human PDEs. Thus PDE-encoding genes of *D. melanogaster* are *CG14940*-PDE1C, *CG8279*-PDE6β, *CG5411*-PDE8A, *CG32648*-PDE9 and *CG10231*-PDE11. Reverse transcriptase–PCRs of adult tissues reveal widespread expression of PDE genes. *Drosophila* Malpighian (renal) tubules express all the six PDEs: *Drosophila* PDE1, *dunce* (PDE4), PDE6, PDE8, PDE9 and PDE11. Antipeptide antibodies were raised against PDE1, PDE6, PDE9 and PDE11. Verification of antibody specificity by Western blotting of cloned and expressed PDE constructs allowed the immunoprecipitation studies of adult *Drosophila* lysates. Biochemical characterization of immunoprecipitated endogenous PDEs showed that PDE1 is a dual-specificity PDE (Michaelis constant K_m for cGMP: 15.3 ± 1 μM; K_m cAMP: 20.5 ± 1.5 μM), PDE6 is a cGMP-specific PDE (K_m cGMP: 37 ± 13 μM) and PDE11 is a dual-specificity PDE (K_m cGMP: 6 ± 2 μM; K_m cAMP: 18.5 ± 5.5 μM). *Drosophila* PDE1, PDE6 and PDE11 display sensitivity to vertebrate PDE inhibitors, zaprinast (IC_{50} was 71 ± 39 μM for PDE1, 0.65 ± 0.015 μM for PDE6 and 1.6 ± 0.5 μM for PDE11) and sildenafil (IC_{50} was 1.3 ± 0.9 μM for PDE1, 0.025 ± 0.005 μM for PDE6 and 0.12 ± 0.06 μM for PDE11). We provide the first characterization of a cGMP-specific PDE and two dual-specificity PDEs in *Drosophila*, and show a high degree of similarity in structure and function between human and *Drosophila* PDEs.

Key words: cGMP-specific phosphodiesterase, *Drosophila melanogaster*, *dunce*, mammalian homologue, sildenafil, zaprinast.

INTRODUCTION

cGMP signalling has been implicated in an increasing number of physiological processes. Recent works on several cell and tissue systems suggest that the enzymes that regulate the breakdown of cGMP, as opposed to its synthesis, are pivotal in maintaining the role of cGMP in cellular function [1–3].

In vertebrates, hydrolysis of cGMP is performed by cyclic nucleotide PDEs (phosphodiesterases), including PDE1, PDE5, PDE6, PDE9, PDE 10 and PDE 11 [4,5]. While some of these, notably PDE5, PDE6 and PDE9, are cG-PDEs (cGMP-specific PDEs), the others are dual-specificity enzymes that hydrolyse both cAMP and cGMP. PDEs are important drug targets, and as such, much is known about the pharmacology and biochemistry of these enzymes. For example, PDE5, the cellular target of sildenafil (Viagra), has been extensively characterized [5].

The use of genetic model organisms (*Drosophila melanogaster* and *Mus musculus*) has been a powerful tool in the demonstration of *in vivo* roles for PDEs [6–8]. However, these studies have focused on the cA-PDEs (cAMP-specific PDEs) and the *Drosophila* PDE, *dunce*, which is a member of the well-characterized PDE4 enzyme family [9]. In *D. melanogaster*, *dunce* mutants exhibit learning defects, while, in mammals, PDE4 selective inhibitors show anti-depressant and anti-inflammatory effects [10,11]. Much less, however, is known about cG-PDE function in an organotypic context, using model organisms. The elegant targeted expression systems available to *Drosophila*, e.g. the GAL4-UAS system (where UAS stands for upstream activating sequence) [12], allow for ectopic expression or disruption of genes of choice in particular cell types or tissues in the intact animal. Thus cell-specific signalling roles of cG-PDE can be assessed in intact tissues [13]. Indeed, we have evaluated cGMP signalling mechanisms *in vivo*, using the genetic model, the *Drosophila* Malpighian (renal) tubule [14]. By doing this, we have shown that cGMP signalling is an important modulator of renal function in *Drosophila* [2,13,15–18]. More specifically, we have shown that cG-PDE activity is critical for tubule function [2,13,17].

The discovery of the key role of *dunce* in learning and memory may have obscured the possibility that other important PDEs exist in the fly. As an important prelude to understand further the roles of cyclic nucleotide PDEs *in vivo*, we have identified and characterized five novel PDEs encoded by the *Drosophila* genome, and show that these are widely expressed in the fly. Specifically, we have identified the novel fly PDEs as PDE1, PDE6, PDE8, PDE9 and PDE11.

Antibodies were raised to PDE1, PDE6, PDE9 and PDE11, and biochemical characterization and inhibitor studies performed for PDE1, PDE6 and PDE11, thus providing the first such characterization of novel *Drosophila* cG-PDE function.

In the present study, we demonstrate conservation of both structure and function between vertebrate and *Drosophila* PDEs and suggest the widespread importance of PDEs in *D. melanogaster*.

EXPERIMENTAL

Drosophila stocks

Stocks were maintained on standard *Drosophila* diet at 25 °C and 55 % humidity, during a 12 h:12 h photoperiod. The *Drosophila*

Abbreviations used: cGK, cGMP-dependent protein kinase; PDE, phosphodiesterase; cA-PDE, cAMP-specific PDE; cG-PDE, cGMP-specific PDE; EST, expressed sequence tag; IP, immunoprecipitation; PAS, Per, ARNT, Sim; PKA, cAMP-dependent protein kinase; RT, reverse transcriptase; UTR, untranslated region.

[1] To whom correspondence should be addressed (email s.a.davies@bio.gla.ac.uk).

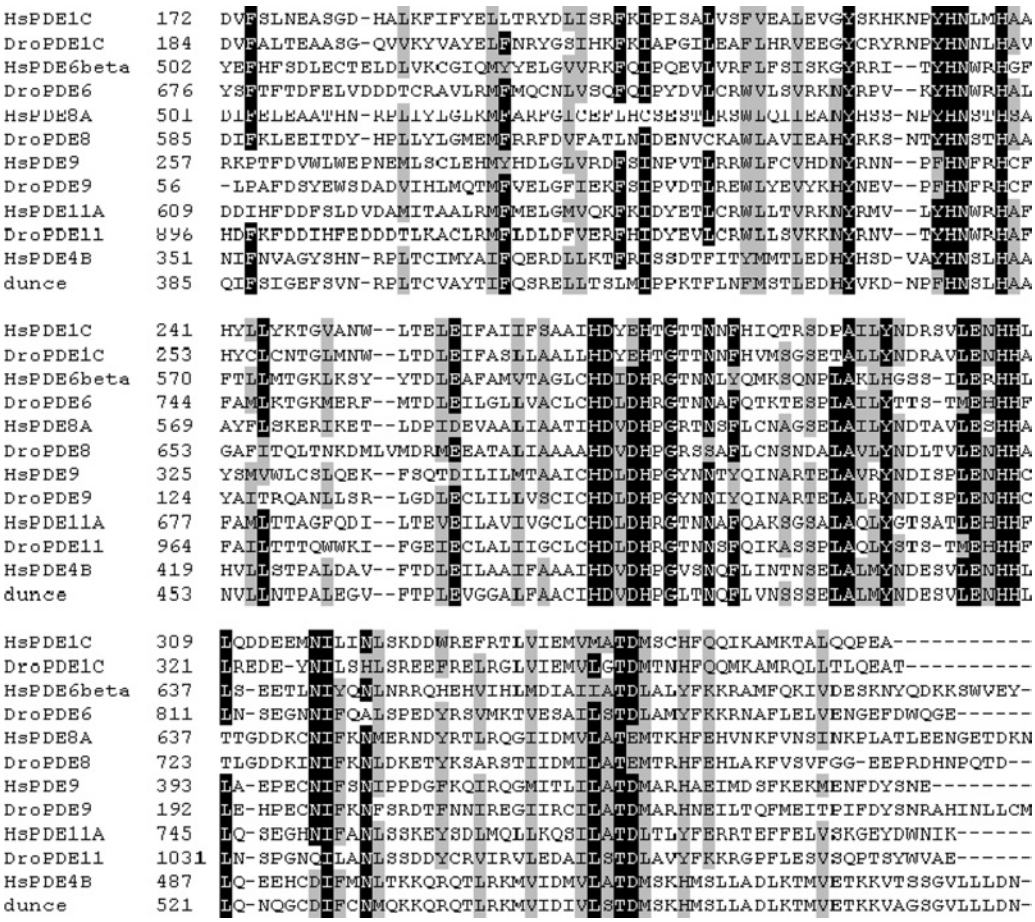

Figure 1 Alignment of the catalytic domains of putative *D. melanogaster* PDEs with *H. sapiens* homologues

The Berkeley *Drosophila* genome project database (now at http://flybase.net/) was searched with representative human PDE protein sequences, and putative *Drosophila* PDEs were identified. Sequence alignments using the *H. sapiens* homologues were performed using ClustalW and drawn using BioEdit. Comparisons of *Drosophila* and human PDEs are shown, where identical residues are shaded black; grey shading indicates residues with 70 % similarity. Complete predicted amino acid sequences for *Drosophila* PDE1, PDE6, PDE8, PDE9 and PDE11 are contained in Supplementary Figure 1 at http://www.BiochemJ.org/bj/388/bj3880333add.htm.

line used in the present study was a standard wild-type strain (Oregon R), used at 7 days post-emergence in all experiments.

Bioinformatics

Polypeptide sequences of the 11 known mammalian PDE gene families were used as probes to obtain the annotated genome sequence of the *D. melanogaster* database. These were submitted to the FLYBLAST server and hits screened for signature $HX_3HX_{21\text{-}23}$D/E 3′-5′ cyclic nucleotide PDE motifs. Alignments of deduced *Drosophila* PDEs were made against relevant human PDEs using ClustalW (http://www.ebi.ac.uk/clustalw/), and drawn using BioEdit (http://www.mbio.ncsu.edu/BioEdit/bioedit.html). In all alignments (Figure 1; also see Supplementary Figure 1 at http://www.BiochemJ.org/bj/388/bj3880333add.htm), residues shaded black are identical, while grey shading indicates similar residues, using a PAM250 scoring matrix at 70 % stringency.

RT (reverse transcriptase)–PCR

Expression of *PDE* genes was confirmed by performing RT–PCR on wild-type fly head and tubule cDNA preparations. Ten *Drosophila* heads or 50 tubules were dissected, poly(A)$^+$ (polyadenylated) RNA was extracted (Dynal mRNA direct kit) and reverse-transcribed with MMLV (Moloney murine leukaemia virus) RNaseH-superscript reverse transcriptase (Invitrogen) as described previously [15]. Reverse transcription reaction mixture (1 μl) was used as a template for PCR containing *PDE* gene-specific primer pairs based on FlyBase sequences (Table 1). Additionally, to control against genomic contamination in cDNA preparations, primers were used which had been designed around

Table 1 Gene-specific primers for *D. melanogaster* PDE genes

Gene-specific primer pairs based on FlyBase sequences of putative genes encoding PDEs (http://fly.ebi.ac.uk:7081/) were used for PCR of adult fly cDNA.

Primer	Sequence 5′–3′
CG8279F	CAAGATTCTGGTCAATGTCGGA
CG8279R	ACAAAAGGTCAAATAGCGGCG
CG10797F	GGAACCAGAAACACTGAGCGAC
CG10797R	TGCGGCTTGCGGAACTTTAG
CG14940F	AGACGCAGGAGAAGAAGAAAAGG
CG14940R	CCAGTTCATCAGACCCGTGTTG
CG10231F	ATGGTCTTCCGCATTCTCACCC
CG10231R	CCTCCACAAAGTTCTCGTCGTTC
CG32648F	GGACTCGTTCTCCTGCCACTATTC
CG32648R	GTTGCCAAAATGACAGCGATTG
CG5411F	CATTGCGAGAACCATTCGTCAC
CG5411R	TTGAAAATCAGGTGCGTGGGGG

intron/exon boundaries. Such primers verified the cDNA quality used in PCRs.

PCR cycle conditions were as follows: 94 °C (2 min), 30 cycles of [94 °C (15 s), 55 °C (30 s), 72 °C (3 min)], 72 °C (10 min). PCR products (400–800 bp) obtained from such RT–PCR experiments were cloned using the Invitrogen Topoisomerase (TOPO TA Cloning) system. Cloned plasmids were purified using Qiagen kits and sequenced to confirm their identity. The cloned PCR products shared 100 % sequence identity with predicted *PDE* transcripts (results not shown).

Anti-PDE antibodies

Polyclonal rabbit anti-peptide antibodies were generated by Genosphere Technologies (Paris, France) against the following C-terminal epitopes for each putative cG-PDE as follows: PDE1, EQAVKDAEARALAT; PDE6, HGSEDSHTPEHQRS; PDE9, MDPDKVSKPGSQVR; and PDE11, PTSTQPSDDDNDAD. Antibodies were affinity-purified before use as described previously [19].

Cloning and expression of PDE1, PDE6 and PDE11 in *Drosophila* S2 cells

Cloning and expression studies were performed using ESTs (expressed sequence tags) as specified, obtained from BDGP (the Berkeley *Drosophila* Genome Project, http://www.fruitfly.org/EST/index.shtml).

PDE1: a full-length EST (RE56844) was available for this gene. All subsequent subcloning was performed using this EST as a template.

PDE6: one EST (GH27433) for PDE6 was available. However, the genome annotation predicted that this EST lacked 271 bp of the 5′-end of the open reading frame. Therefore an RT–PCR strategy was used to obtain the full-length open reading frame. A forward PCR primer (PDE6ORFF) was designed complementary to the 5′-end of the open reading frame. To establish whether or not the PDE6 transcript extended to the 5′-end of the predicted open reading frame, the reverse primer (PDE6R673) was designed to span the first intron, thus enabling the distinction to be made between amplification from genomic DNA versus cDNA. RT–PCR was then performed using gene-specific cDNA synthesized from total head RNA primed with the reverse primer as a template. This produced a fragment of the expected size, which was cloned and sequenced to confirm that it represented the 5′-end of the PDE6 transcript. The full-length open reading frame was then assembled using fusion PCR, in which the separate open reading frame moieties were amplified in two PCRs. The PCR products were purified and used in equal amounts as templates in a further PCR experiment using PDE6ORFF and PDE6ORFR primers. This gave a single product comprising the full-length open reading frame of PDE6, with an in-frame stop codon occurring at the 5′-end of 57 bp to the predicted ATG start codon. Northern blotting using a digoxigenin-labelled riboprobe complementary to the 3′-UTR (3′-untranslated region) of PDE6 showed that the full-length PDE6 transcript (~7 kb) is detectable in both head and body total RNA (results not shown). The full-length open reading frame was sequenced to check for PCR errors and PCR artifacts, and the construct (pCR2.1PDE6ORF) was used as a template in all subsequent subcloning procedures.

PDE9: no ESTs were available for PDE9. However, as it is possible to characterize PDEs from cloned catalytic constructs alone [20], primers (PDE9catF and PDE9catDESR) were designed to encompass the catalytic domain of PDE9. Using the Malpighian (renal)-tubule-specific template cDNA, a fragment of the expected size was amplified and verified, and used for all subsequent cloning.

PDE11: initially, two incomplete ESTs coding for PDE11 were available from BDGP (RH43346 and LP04047). These encoded the 3′-UTR, including a poly(A)$^+$ tail and approximately half of the coding sequence of *CG10231*. Library screening and 5′-rapid amplification of cDNA ends were used to obtain the full-length sequence for *CG10231*. However, a newly released EST, SD13096, was found to encode the full-length PDE11 (see Supplementary Figure 1 at http://www.BiochemJ.org/bj/388/bj3880333add.htm). This was used for subsequent cloning; however, expression of PDE11 by this construct in S2 cells proved to be difficult (results not shown). Therefore to achieve the expression of PDE11 for validation of the anti-PDE11 antibody (Figure 4), a construct comprising the sequence for the PDE11 catalytic domain and the C-terminal region was used. This 2130 bp gene fragment was amplified using a forward primer 5′ to the catalytic domain (PDE11catF 5′-ATGGAGGCGTTCGCCATCTTC-TGC-3′) and a reverse primer at the 3′-end of the open reading frame omitting the stop codon (PDE11V5R5′-TTTTTCAACCG-CCATAGCGG-3′). The fragment was cloned into the S2 cell expression vector pMT V5 His TOPO (below) and the resultant constructs were screened for the correct orientation of the insert.

All PDE constructs for cloning were sequence-verified and cloned into expression vector pMT/V5-HIS-TOPO (Invitrogen). This vector incorporates the C-terminal V5 epitope-tag [GKPIPN-PLLGLDST, derived from a small epitope (Pk) present on the P and V proteins of the paramyxovirus of SV5 (simian virus 5)] and His_6 tag. These plasmids were then used for the transient transfection of S2 cells under conditions of Cu^{2+}-inducible expression. Cells were cultured according to standard methods described in [21]. Approximately 3×10^6 cells were used in each transfection, which was performed using calcium phosphate according to standard techniques (Invitrogen); transfection efficiencies were routinely 10 %.

Western-blot analysis

Samples of 3×10^6 *PDE1*-, *PDE6*-, *PDE9*- and *PDE11*-transfected S2 cells were collected by centrifugation at 5000 ***g*** for 3 min. Cells were resuspended in PBS, spun down once more and resuspended in lysis buffer {50 mM Tris (pH 7.5), 150 mM NaCl, 1 % (v/v) Igepal CA-630 [octylphenyl-poly(ethylene glycol); Sigma] and 1 μg/ml protease inhibitor cocktail with PMSF (Sigma)}. Cells were disrupted by sonication and centrifuged at 15000 ***g*** for 5 min, and the supernatants were collected. The protein content of each sample was estimated using the Bradford assay. Samples (10 μg of protein each) were loaded on to each lane for Western-blot analysis, performed according to standard methods described in [13] using the ECL® system (Amersham Biosciences). Blots were probed with anti-V5-epitope antibody (1/5000) (Invitrogen) or rabbit polyclonal anti-PDE antibodies (1/400). Horseradish peroxidase-conjugated secondary antibodies (Amersham Biosciences) were used at a concentration of 1/5000. This procedure was also performed for untransfected (control) cells for blotting with anti-PDE antibodies.

IP (immunoprecipitation) assays and cG-PDE assays

IP assays were performed from heads of 7–9-day-old wild-type (Oregon R) adult *Drosophila*. For each IP sample, 20 heads were dissected and homogenized in 1 ml of lysis buffer [10 %, v/v, glycerol, 1 %, v/v, Triton X-100, 150 mM NaCl and 50 mM Hepes (pH 7.5), with 10 μl of protease inhibitor cocktail]. Samples were centrifuged at 15000 ***g*** at 4 °C for 5 min to remove insoluble material and the supernatant was removed to a fresh tube. Samples were precleared by an end-over-end incubation for 1 h at 4 °C with 25 μl of Protein A–Sepharose beads (Sigma) that had been prewashed with lysis buffer. Beads were pelleted by centrifugation

Table 2 Assignment of *D. melanogaster* homologues of vertebrate PDEs

Sequence information for novel PDE genes and deduced proteins identified from the *D. melanogaster* genome is listed, together with closest human homologues. Full-length ESTs for *Drosophila* PDE genes are also listed, where available (http://www.fruitfly.org/EST/index.shtml); except for GH27433*, which is not full-length. The percentage identities and similarities for each gene are calculated over the length of the shorter (human) homologue, and also in relation to the catalytic domain.

Gene	Human homologue	Percentage amino acid identity (similarity)		Predicted length of polypeptide (amino acids)	ESTs
		Human homologue	Catalytic domain		
CG14940	PDE1	40 (56)	63 (79)	1818	RE56844
CG8279	PDE6	28 (46)	51 (69)	1131	GH27433*
CG5411 transcript A	PDE8	34 (52)	60 (79)	914	SD18711
CG5411 transcript B	PDE8	35 (53)	60 (79)	904	RE31467
CG5411 transcript C	PDE8	47 (66)	60 (79)	400	GH21295
CG5411 transcript D	PDE8	37 (57)	60 (79)	805	RE35136
CG5411 transcript E	PDE8	34 (52)	60 (79)	914	RE07805
CG5411 transcript F	PDE8	23 (9)	60 (79)	400	LD46553
CG32648	PDE9	26 (34)	63 (76)	2080	None
CG10231	PDE11	38 (55)	77 (96)	1545	SD13096

at 5000 ***g*** at 4 °C for 1 min and the supernatant was removed to a fresh tube. Samples were then incubated with 5 μg of PDE-specific antibody or 5 μg of IgG control (Sigma) with an end-over-end mixing at 4 °C for 1 h. Protein was then precipitated by adding 10 μl of prewashed Protein A beads. After 30 min of incubation at 4 °C with mixing, beads were pelleted by centrifugation, washed three times with 0.5 ml of lysis buffer, followed by three washes with ice-cold KHEM buffer (50 mM KCl, 50 mM Hepes, pH 7.2, 10 mM EGTA and 1.92 mM $MgCl_2$). Samples were assayed for PDE activity as described previously [22] in the presence of substrate and other appropriate reagents as described in the legends of Figures 5–7. Results are expressed as PDE activity: cGMP or cAMP hydrolysed $\cdot$ (IP assay)$^{-1}$ $\cdot$ min^{-1}, mean $\pm$ S.E.M., $n = 3$–6. Where appropriate, statistically significant data are indicated by $^{*}P < 0.05$ (Student's t test, unpaired samples).

RESULTS

The *D. melanogaster* genome encodes five novel putative PDEs

Using the mammalian vertebrate sequences for comparison and the $HX_3HX_{21\text{-}23}D/E$ protein cyclic nucleotide PDE motif as bait in an *in silico* screen, we identified five genes encoding putative novel PDEs in the *Drosophila* genome (Table 2). This was in addition to the previously characterized cAMP-PDE, *dunce* (Table 2). Homologues to mammalian PDE1, PDE6, PDE8, PDE9 and PDE11 were identified based on sequence similarity within the predicted catalytic domain, as well as by the presence of sequences proposed to be regulatory and post-translational modification sequences in the vertebrate enzymes [23]. Comparison of the *Drosophila* PDE predicted protein sequences with their mammalian homologues revealed high sequence identity (51–77 %) within the conserved catalytic region (Table 2). Lower sequence identity (28–40 %) was found over the complete protein sequence (Table 2).

The five putative *Drosophila* PDEs contain domains and motifs homologous with their mammalian counterparts

An alignment was made of the catalytic domains of each *Drosophila* PDE with its human homologue (Figure 1), where *dunce* was included as a positive control. Inspection of the deduced protein sequences (Figure 1) reveals that each putative PDE encodes the signature $HX_3HX_{21\text{-}23}D/E$ metal-dependent hydrolase motif [23]. Comparison of *Drosophila* with human PDEs confirms the high percentage of sequence identity within the catalytic domain (Table 2).

Drosophila PDE1

Although calcium (Ca^{2+})/calmodulin-sensitive dual-specificity PDE activity has been determined in *Drosophila* [24], its molecular identity was unknown. In the present study, we show that *CG14940* encodes the closest *Drosophila* homologue of the mammalian Ca^{2+}/calmodulin-sensitive PDE, PDE1. It shares 40 % overall amino acid identity with mammalian PDE1C, but 63 % identity with the conserved catalytic domain (Figure 1). The N-terminal autoinhibitory motif of mammalian PDE1A [25] appears to be conserved between mammals and flies; however, only one of the two mammalian calmodulin-binding sites appears to be present in *Drosophila* PDE1 (Figure 2). The EST sequence for *CG14940* (RE56844) provides strong evidence that *Drosophila* PDE1 has an open reading frame of 1815 nucleotides, which encodes a polypeptide of 605 amino acids. Sequence comparisons between *Drosophila* PDE1 and *Homo sapiens* PDE1C revealed that the fly gene encodes an extra 13 amino acids at the N-terminus and is truncated by 133 amino acids at the C-terminus (see Supplementary Figure 1 at http://www.BiochemJ.org/bj/388/bj3880333add.htm). Since no study has uncovered a role for the C-terminal region of PDE1, the significance of this latter finding is unknown.

Recent structural studies have illuminated the mechanism behind PDE substrate-specificity, where a conserved glutamine residue changes orientation with respect to the bound substrate (the 'Q switch' mechanism) [20]. The residues surrounding this glutamine residue, in particular critical histidine residues, confer this rotational freedom, which is supposed to form the basis of mechanism of action of dual-specificity PDEs. This glutamine residue (Gln-426 in PDE1C and Gln-439 in *Drosophila* PDE1), which co-ordinates the nucleoside purine, was identified from sequence alignments between the catalytic domains of the *Drosophila* and *H. sapiens* PDEs (see Supplementary Figure 1 at http://www.BiochemJ.org/bj/388/bj3880333add.htm). Three other critical residues surrounding this glutamine residue, His-381, His-373 and Trp-496 in mammalian PDE1C, are conserved in *Drosophila* PDE1 (the corresponding residues are His-399, His-391 and Trp-539). It therefore appears that *CG14940* has the structural correlates required to encode dual-specificity PDE1 activity in *D. melanogaster*.

Drosophila PDE6

The deduced protein encoded by *CG8279* shares 28 % overall sequence identity with mammalian PDE6β, but shows 51 % identity within the catalytic domain. However, it appears to be more

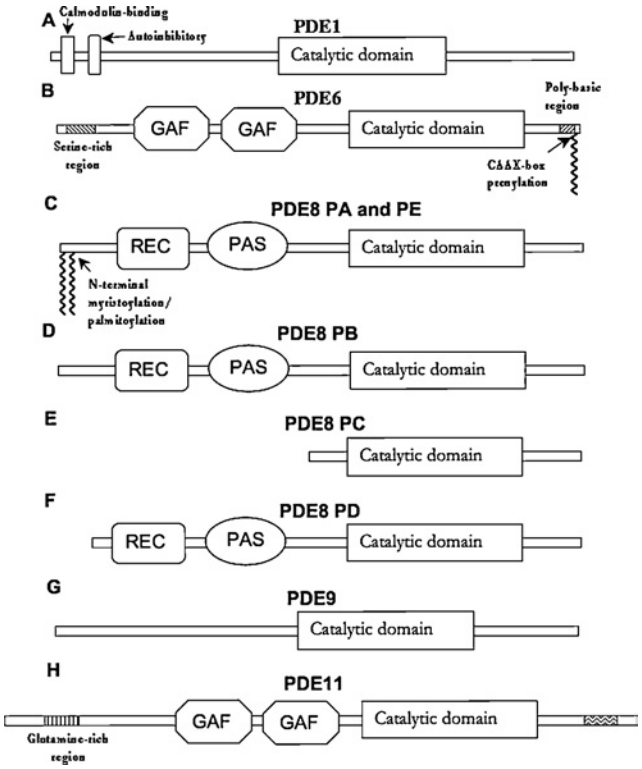

Figure 2 Schematic diagram of novel *Drosophila* PDEs

Schematic representations of deduced protein sequences are derived from ClustalW alignments. These were made for each putative *Drosophila* PDE: (**A**) PDE1, (**B**) PDE6, (**C**–**F**) PDE8, (**G**) PDE9 and (**H**) PDE11 with their closest mammalian homologue, as ascertained by lowest BLAST expect score and closest overall sequence similarity.

similar to mammalian PDE5 (58 % identity within the catalytic domain, Table 2), which suggests that *CG8279* may encode an ancestral form of mammalian PDE5. Interestingly, one of the most prominent features of the predicted protein sequence of *CG8279* is the presence of a C-terminal CAAX-box prenylation motif (Figure 2, and see Supplementary Figure 1 at http://www.BiochemJ.org/bj/388/bj3880333add.htm). This and the presence of conserved catalytic-domain residues led to its designation as a PDE6 homologue. The DNA sequence predicted by the genome annotation comprises a 3393 bp open reading frame, coding for a polypeptide of 1131 amino acids. One EST, GH27433, comprising bp 271 of the predicted open reading frame to a poly(A)$^+$ tail 1.6 kb downstream of the TGA stop codon, was available (BDGP). Further cloning and sequencing work (see the Experimental section) verified the *Drosophila* genome annotation for *CG8279*.

Drosophila PDE6 contains regions similar to the tandem cGMP-binding and dimerization mediating GAF domains [23,26] that are found within the N-terminal region of several mammalian PDEs (Figure 2). Proximal to the C-terminal CAAX-box prenylation motif lies a polybasic region comprising four lysine, one arginine and two serine residues, and also contains a consensus cGK (cGMP-dependent protein kinase) or PKA (cAMP-dependent protein kinase) phosphorylation motif (KKRS). Another cGK/PKA phosphorylation motif (KRPS) occurs at predicted amino acids 197–200. This second phosphorylation motif may be homologous with that of mammalian PDE5, which also lies N-terminal to the GAF domains and is supposed to modulate the binding of cGMP to these regulatory domains [23]. Comparison of *Drosophila* PDE6 polypeptide with *H. sapiens* PDE6β shows that the former has an extra 99 amino acids at the N-terminus and a 111-amino-acid insertion between the end of the catalytic domain and the prenylation motif (see Supplementary Figure 1 at http://www.BiochemJ.org/bj/388/bj3880333add.htm).

The canonical vertebrate cG-PDE, PDE5A, specifically hydrolyses cGMP. Structural studies have uncovered the main mechanism conferring cGMP-specificity on PDE5A [20]. This involves a key Gln-817 that is orientated to form a clamp by hydrogen-bonding interactions between Gln-817 and Gln-775 and also by hydrogen bonds between the carboxyl backbone of Ala-767 and Gln-775, and Trp-853 and Gln-775. Each of these residues is conserved in *Drosophila* PDE6 (Q935, Q893, A885 and W970) and indeed in mammalian PDE6β, another cG-PDE (see Supplementary Figure 1 at http://www.BiochemJ.org/bj/388/bj3880333add.htm). This suggests that *Drosophila* PDE6 is a cG-PDE.

Drosophila PDE8

The predicted polypeptide sequence of the gene *CG5411* bears close resemblance to human PDE8, sharing 30 % overall amino acid sequence identity and 60 % identity within the catalytic domain (Table 2 and Figure 1). At the N-terminus is a six-amino-acid consensus myristoylation/palmitoylation motif, MGCAP, which is almost identical with that contained in human PDE8A1 (see Supplementary Figure 1 at http://www.BiochemJ.org/bj/388/bj3880333add.htm). *N*-myristoyltransferase strictly requires a glycine residue at position 2 and a preference for serine or threonine residue at position 6; therefore MGCAPS represents a strong consensus sequence for this enzyme [27]. Palmitoylated proteins fall into three categories; one group comprises transmembrane proteins that are acylated near the membrane; the second group of proteins, typified by the Ras family, is modified near the C-terminus; and the third group is modified at the N-terminus. PDE8 falls into the last category; the cysteine residue at position 3 is a prime candidate for post-translational palmitoylation. The close conservation between mammalian and fly PDE8 at the N-terminus suggests that lipid modification is important for the function of both proteins.

The predicted polypeptide sequence of *CG5411* also possesses two conserved domains N-terminal to the catalytic domain. First, a REC (recA) domain, which shows 38 % identity and 54 % similarity with human PDE8A REC domain, was identified as a phosphate acceptor domain in the bacterial two-component system [28]. Secondly, there is a PAS (Per, ARNT, Sim) domain (34 % identity and 53 % similarity with human PDE8) that has been shown to serve several functions, including circadian cycling, dimerization and mediation of protein–protein interactions [29]. Taking into account all of these similarities, *CG5411* was designated as the *Drosophila* PDE8 homologue.

The predicted nucleotide sequence of *Drosophila* PDE8 had 19 exons and covers over 13 kb of genomic sequence. To confirm the predicted nucleotide sequence, ESTs were obtained. Three ESTs, which have been sequenced at the 5′- and 3′-ends, were identified, which matched the PDE8 predicted nucleotide sequence. They were GH21295, LD46553 and SD18711 (Table 2). The sequence of GH21295 comprised a short 280 bp region immediately 5′ from the predicted 13th exon, whilst the poly(A)$^+$ tail occurred 1.35 kb 3′ to the putative stop codon (Table 2). At 30 bp upstream from the poly(A)$^+$ tail is a poly(A)$^+$ signal sequence (ATAAA). EST LD46553 comprises the same transcription start site as GH21295 yet had 2.1 kb of sequence between the putative stop codon and the poly(A)$^+$ tail (Table 2). SD18711 encoded the full predicted nucleotide sequence, in addition to 320 bp of 5′-UTR, resulting in an open reading frame of 3180 bp, which translates into a polypeptide of 1060 amino acids.

Since this analysis was performed, version 3 of the *Drosophila* genome annotation (http://flybase.net/annot/) was released. This has identified five transcripts encoding four different polypeptides for PDE8 (Figure 2), in which the open reading frames of transcripts A and E are identical. Analysis of LD46553 suggests that a further transcript exists, identical with transcript C with an 800 bp extension to the 3′-UTR, designated as transcript F. Transcripts B, C and D do not encode the N-terminal myristoylation/palmitoylation motif (Figure 2). Interestingly, all seven splice forms of *H. sapiens* PDE8A and PDE8B do encode this motif. Transcript C encodes neither the PAS nor REC domain, being truncated near the N-terminus of the catalytic domain (Figure 2). Transcripts A, B, C and D all encode unique N-terminal sequences. Since the N-terminal regions of several PDEs have been shown to account for their differential localization and choice of interacting partner, this was of particular interest. Therefore PSORT (http://psort.nibb.ac.jp/) predictions for the subcellular localization of each PDE8 isoform were made. Proteins A, C and D were predicted to be cytoplasmic, whereas Protein B was predicted to be confined to mitochondria.

Mammalian PDE8 is a high-affinity cAMP-specific PDE [30,31]. However, the crystal structure of this PDE has not been reported. Comparison of mammalian PDE8 with the structure of the cAMP-specific PDE4B suggests that two residues, the conserved Gln-369 and Asn-321, make contact with the substrate adenine. The conserved residue corresponding to Asn-321 in *Drosophila* PDE8 is Asn-729, which could possibly interact with the substrate in a similar way to PDE4B. Moreover, each of the four residues within the nucleoside-binding pocket is conserved between *Drosophila* PDE8 and human PDE8: Asn-803, Cys-811, Gln-851 and Trp-885 in *Drosophila* PDE8, corresponding to Cys-729, Asn-737, Gln-778 and Trp-812 in human PDE8A. This would suggest that *Drosophila* PDE8 could possess the same substrate-specificity as human PDE8A.

Drosophila PDE9

The catalytic domain of mammalian PDE9 shows low sequence identity (29–35 %) with other mammalian PDEs [32]. However, the predicted polypeptide sequence encoded by *Drosophila* gene *CG32648* shows 63 % amino acid identity within the catalytic domain (Figure 1). Therefore *CG32648* was designated as *Drosophila* PDE9. PDE9 shows no sequence similarity to *Drosophila* PDE9 outside of the catalytic domain. This may indicate that the sequence annotation does not represent the actual gene structure. However, as no ESTs were available for study, it is not possible at this stage to verify the PDE9 sequence.

Drosophila PDE11

Alignment of the predicted polypeptide sequence of *CG10231* with mammalian PDE11A showed that these genes are closely related. Sequence identity within the catalytic domain is 77 %, although the overall sequence identity is 38 % (Figure 1 and Table 2). Like human PDE11, the predicted polypeptide sequence of *CG10231* contains tandem GAF domains at the N-terminal region (Figure 2). Because of this close similarity to human PDE11A (see Supplementary Figure 1 at http://www.BiochemJ.org/bj/388/bj3880333add.htm), *CG10231* was designated as *Drosophila* PDE11. Interestingly, PDE5, which is phosphorylated by cGK [33], contains one cGK phosphorylation motif in each subunit [34]. We have identified four such consensus motifs in PDE11 (see Supplementary Figure 1 at http://www.BiochemJ.org/bj/388/bj3880333add.htm). Although this does suggest that PDE11 may be a substrate for cGK in *Drosophila*, the significance of four putative phosphorylation sites is currently unknown.

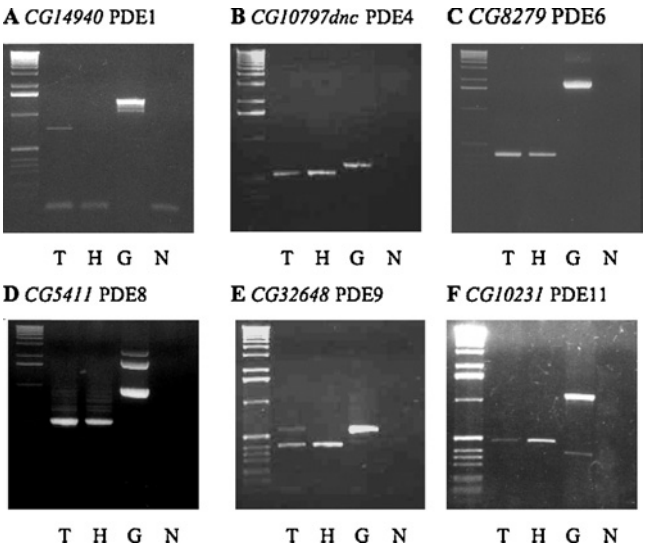

Figure 3 PDE gene expression in adult *D. melanogaster*

RT–PCR using cDNA templates from tubule (T), head (H), and control genomic DNA (G) using intron-spanning gene-specific primers for putative PDE-encoding genes. (N) No template control. In all gels, the first lane is a 1 kb DNA ladder (Invitrogen). Expected PCR products indicated were obtained for all putative PDE genes: (**A**) *CG14940* (PDE1C), genomic-1438 bp and cDNA-743 bp; (**B**) *CG10797* (*dnc*) (PDE4), genomic-603 bp and cDNA-438 bp; (**C**) *CG8279* (PDE6), genomic-1969 bp and cDNA-406 bp; (**D**) *CG5411* (PDE8), genomic-998 bp and cDNA-506 bp; (**E**) *CG32648* (PDE9), genomic-567 bp, cDNA-391 bp; (**F**) *CG10231* (PDE11), genomic-1118 bp and cDNA-472 bp. PCR products were cloned and sequenced and found to have 100 % identity with PDE genes (results not shown).

When this study was initiated, two incomplete ESTs (LP04097 and RH43346) were available from BDGP. RH43346 provided the longest sequence, encoding the last six predicted exons, part of the seventh exon and a 3′-UTR of 1.6 kb with a poly(A)$^+$ tail and poly(A)$^+$ signal sequence.

However, a newly released EST, SD13096, was found to encode the full-length PDE11 (Supplementary Figure 1). Northern blotting of RNA from adult heads and bodies using a digoxigenin-labelled riboprobe, complementary to the 3′-UTR of SD13096, showed that the PDE11 transcript was approx. 5.8 kb long, the same length as SD13096 (results not shown), confirming that SD13096 encodes a full-length cDNA.

Widespread expression of PDE genes in adult tissue

Using RT–PCR, we investigated the expression of the putative PDE genes in tissues of interest, i.e. in adult head and Malpighian tubules. Results in Figures 3(A)–3(F) show widespread expression of all the PDEs. Interestingly, expression of PDE6 in *Drosophila* is widespread and is not confined to the eye tissue, as is mammalian PDE6.

Although *CG32648* expression in the head by RT–PCR using gene-specific primers (see the Experimental section) is not documented, this gene is expressed in a head cDNA library (GH library, Berkeley *Drosophila* genome project http://www.fruitfly.org/EST/; results not shown). Expression of PDE9 in adult *Drosophila* tissues is further confirmed by microarray analysis using Affymetrix arrays [35].

Microarray analysis of PDE gene expression in both tubules and in the rest of adult flies confirms the expression data using gene-specific primers (Figure 3). In particular, *CG8279*-PDE6, *CG5411*-PDE8 and *CG10231*-PDE11 are all significantly enriched in tubules compared with the rest of the fly (http://www.mblab.gla.ac.uk/%7Ejulian/arraysearch.cgi).

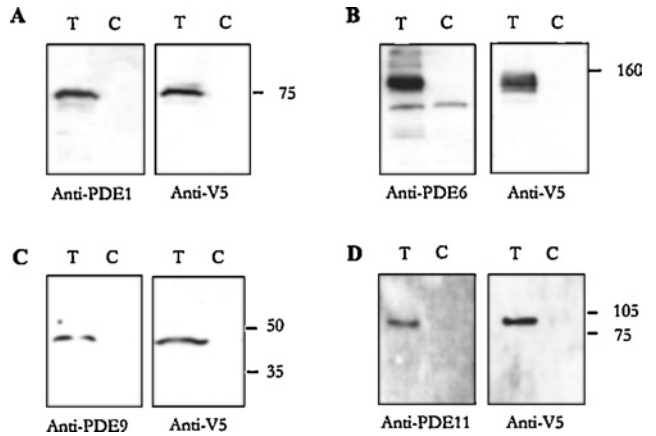

Figure 4 Anti-PDE antibodies recognize specific PDEs

V5-tagged constructs for PDE1, PDE6, PDE9 and PDE11 were transfected into S2 cells, and cell extracts prepared from transfected cells (T) and untransfected controls (C). Western blotting was performed with cell extracts using polyclonal anti-PDE antibodies. Left panel: (**A**) PDE1, (**B**) PDE6, (**C**) PDE9 and (**D**) PDE11. Right panel: anti-V5 antibody [18] (**A**–**D**) PDE1–PDE11, same as left panel. Bands identified by both anti-PDE and anti-V5 antibodies in samples from transfected but not control cells were as follows: PDE1: 75 kDa; PDE6: 150 kDa; PDE9: 47 kDa; PDE11: 100 kDa, indicated by use of molecular mass standards (kDa).

This confirms the importance of cyclic nucleotide signalling in *Drosophila* renal function. Finally, given that at least three of the expressed genes are putative cG-PDEs (*CG8279*-PDE6, *CG14940*-PDE1C and *CG32648*-PDE9), this suggests that regulation of cGMP signalling is necessarily complex, even in this simple epithelium.

Multiple cG-PDEs in *D. melanogaster*

To perform biochemical characterization of the PDEs encoded by the identified PDE genes, cloning and expression studies were attempted. Cloning of the full-length open reading frames of PDE1, PDE6, PDE8, PDE11 as well as the PDE9 catalytic domain was performed; although expression of all these constructs in *Drosophila* S2 cells was achieved, with the exception of PDE6 [36], obtaining active recombinant enzymes in S2 extracts from transfected cells proved to be highly problematic. We currently do not have a good explanation for this. The lack of activity associated with the PDE protein expressed in this model system may be associated with incorrect processing in *Drosophila* S2 cells, a macrophage-like line. Indeed, it could be due to the lack of appropriate chaperones or scaffolding partners in these cells that are required for folding, such as those identified for vertebrate PDEs, and needed to form a catalytically competent enzyme [20,37–39]. Therefore another approach was used to characterize the *Drosophila* PDEs, in particular putative cG-PDEs and dual-specificity PDEs. Polyclonal antibodies were raised to the unique C-termini of PDE1, PDE6, PDE9 and PDE11. Successful expression of recombinant protein for PDE1, PDE6, as well as the catalytic domain of PDE9 and catalytic domain plus C-terminal region of PDE11 in S2 cells, allowed antibody specificity to be verified by Western blotting (Figure 4). Expected sizes of polypeptides were obtained for each PDE construct.

Successful generation of PDE-specific antibodies allowed biochemical characterization of novel PDE1, PDE6 and PDE11 from immunoprecipitated samples of adult *Drosophila* head extract, subjected to PDE assays.

The lack of PDE activity from immunoprecipitated samples using control IgG fraction, compared with PDE activity obtained using anti-PDE antibodies (Figure 5), further confirms the

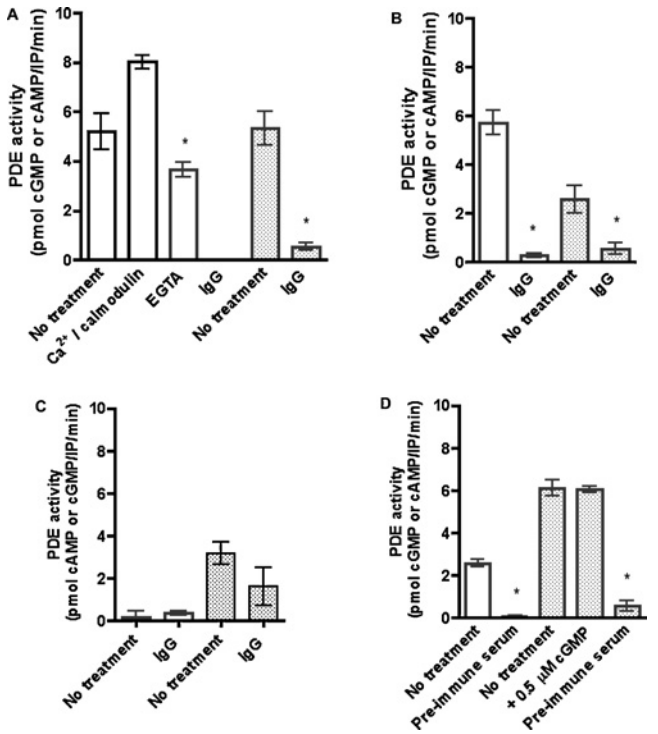

Figure 5 PDEs encoded by *Drosophila* PDE genes exhibit cG- and cA-PDE activity

PDEs were immunoprecipitated from adult *Drosophila* head lysates using affinity-purified antibodies (PDE1, PDE6 and PDE9) and whole serum (PDE11). Control IPs were performed with IgG (preimmune serum for PDE11). Each immunoprecipitated sample was assayed for cGMP- and cAMP-specific PDE activity, where cG-PDE activity is indicated by unshaded bars; and cAMP-PDE activity is indicated by shaded bars. For each PDE, activities were assessed under the conditions described in the *x*-axis for each graph: (**A**) PDE1, (**B**) PDE6, (**C**) PDE9 and (**D**) PDE11. PDE activities were assayed at either 10 μM cGMP (for cG-PDE activity) or 10 μM cAMP (for cA-PDE activity). Ca^{2+}/calmodulin-stimulated PDE1 activity was assayed at 0.2 mM Ca^{2+} and 0.4 mg/ml calmodulin. Data are represented as PDE activity [pmol of cGMP or cAMP $\cdot$ (IP assay)$^{-1}$ $\cdot$ min^{-1} $\pm$ S.E.M., $n = 6$]. cG-PDE activity in the IgG-treated fraction from PDE1 samples (**A**) was negligible. *, Data statistically significant between antibody-specific and control IPs, assayed for cG- and cA-specific PDE activity, where $P < 0.05$ (Student's unpaired *t* test). Additionally, in PDE1 panel, * indicates statistical significance ($P < 0.05$, Student's unpaired *t* test) between EGTA-treated (0.1 mM EGTA) and untreated samples assayed for cG-PDE activity.

specificity of these antibodies. Figure 5(A) demonstrates that PDE1 hydrolyses both cGMP and cAMP when assayed at a substrate concentration of 10 μM. As expected by sequence identity, PDE1 is a Ca^{2+}/calmodulin-regulated enzyme. We show that cG-PDE activity is inhibited by the calcium chelator EGTA, but is stimulated by the addition of 0.2 mM Ca^{2+} and 0.4 mg/ml calmodulin.

PDE6 displays cG-PDE activity at 10 μM cGMP; however, significant cAMP-specific PDE activity was also found (Figure 5B). However, assay of PDE6 activity from transfected *Drosophila* S2 cells does not reveal cA-PDE activity [36].

PDE11 hydrolyses both cGMP and cAMP (Figure 5D). Interestingly, cAMP hydrolysis was not augmented by the addition of 0.5 μM cGMP to the assay mix.

PDE9 activity was not recovered successfully from immunoprecipitated samples using PDE9-specific antibody (Figure 5C). Although a small amount of cAMP-PDE activity was recovered, this activity was not statistically significant when compared with IgG controls. Thus all further characterization was performed for PDE1, PDE6 and PDE11 only.

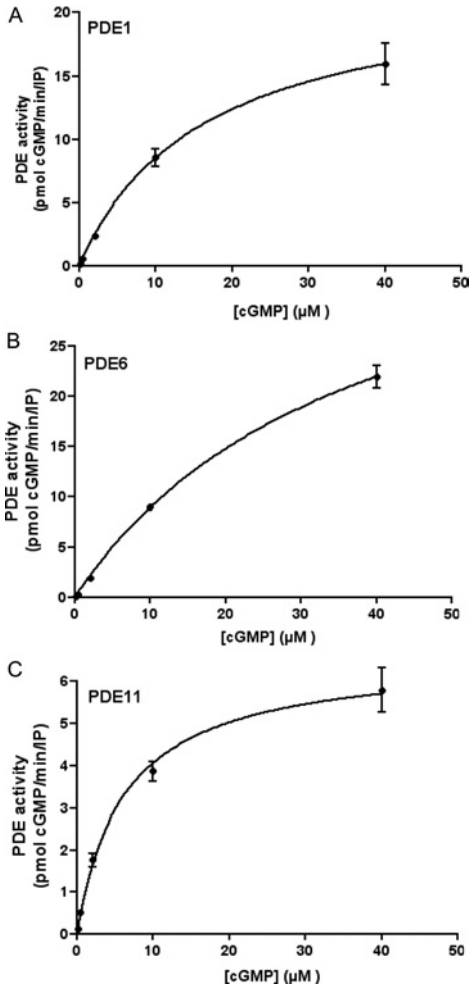

Figure 6 Kinetic analysis of *Drosophila* cG-PDEs

Kinetics of cG-PDE activity in immunoprecipitated samples from *Drosophila* head lysate using antibodies raised against three novel putative *Drosophila* PDEs. cG-PDE assays were performed at five substrate concentrations: 0.5, 2, 4, 10 and 40 μM cGMP. (**A**–**C**) Best-fit square-hyperbola non-linear regression plots. K_m values calculated from analysis of the data (GraphPad Prism4) are shown in the text. (**A**) PDE1, (**B**) PDE6 and (**C**) PDE11. Results are expressed as cG-PDE activity [pmol of cGMP hydrolysed · (IP assay)$^{-1}$ · min^{-1} $\pm$ S.E.M., $n = 3$].

Biochemical characteristics of novel *Drosophila* PDEs

Figure 6 shows cGMP dependence of PDE1 (panel A), PDE6 (panel B) and PDE11 (panel C) activities. Values of the Michaelis constant K_m were determined by non-linear regression plots (Figure 6) and confirmed by Lineweaver–Burk analysis (results not shown). PDE1 displayed a K_m of 15.3 $\pm$ 1 μM (15 μM by Lineweaver–Burk analysis) for cGMP; PDE6 showed a K_m of 37 $\pm$ 13 μM (50 μM by Lineweaver–Burk analysis), whereas PDE11 had a K_m of 6 $\pm$ 2 μM (4.6 μM by Lineweaver–Burk analysis). Although PDE6 activity could have been assayed at higher substrate concentrations, the approximate K_m deduced from data shown in Figure 6(B) is in agreement with that obtained by analysis of PDE6 kinetics in PDE6-transfected S2 cell extracts [36].

Taken together, our kinetic data show that PDE11 is the *Drosophila* PDE with highest cGMP affinity among the PDEs analysed so far. These values also confirm the idea that *Drosophila* cG-PDEs are enzymes with high K_m values, as these are in close agreement with previous data for cG-PDE activity assayed in *Drosophila* renal tubule extracts, which show a K_m of 15.88 $\pm$ 10.22 μM for cGMP [13].

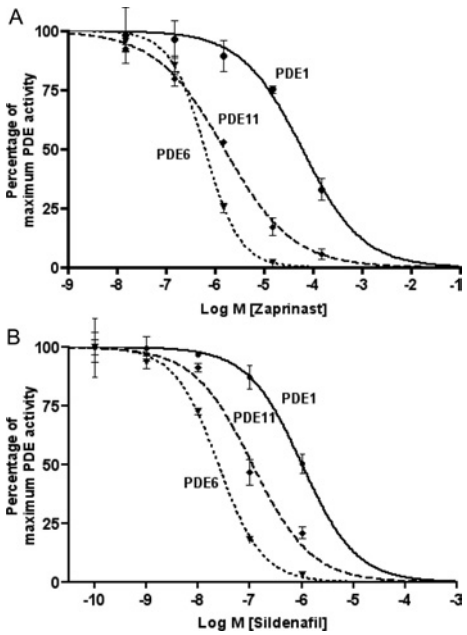

Figure 7 Inhibition of *Drosophila* PDEs by zaprinast and sildenafil

Immunoprecipitated samples from *Drosophila* head lysates using antibodies specific for PDE1, PDE6 and PDE11 were assayed for cG-PDE activity [pmol of cGMP hydrolysed · (IP assay)$^{-1}$ · min^{-1} $\pm$ S.E.M. at 10 μM substrate concentration] in the absence (control) or in the presence of 1.5×10^{-9}, 1.5×10^{-8}, 1.5×10^{-7}, 1.5×10^{-6}, 1.5×10^{-5} and 1.5×10^{-4} M zaprinast (**A**), and 10^{-10}, 10^{-9}, 10^{-8}, 10^{-7} and 10^{-6} M sildenafil citrate (**B**). To aid comparison, results are expressed as percentage of maximum (control) PDE activity $\pm$ S.E.M., $n = 3$. Control PDE activity [pmol of cGMP hydrolysed · (IP assay)$^{-1}$ · min^{-1} $\pm$ S.E.M.] for PDE1: 2.95 $\pm$ 0.16; PDE6: 11.11 $\pm$ 0.195; and PDE11: 3.65 $\pm$ 0.15.

Similar kinetic experiments performed for cAMP-dependent activity for PDE1 and PDE11 showed that PDE1 displayed a K_m of 20.5 $\pm$ 1.5 μM, whereas PDE11 has a K_m of 18.5 $\pm$ 1.5 μM for cAMP (results not shown).

Previous work has shown that cG-PDE activity in *Drosophila* renal tissue is sensitive to inhibitors of vertebrate cG-PDEs, for example zaprinast [2] and the PDE5-specific inhibitor, sildenafil [13]. In the present study, we show that isolated cG-PDE activities are sensitive to both these inhibitors (Figures 7A and 7B).

PDE1 is inhibited by zaprinast, with an IC_{50} value of 71 $\pm$ 39 μM (Figure 7A), and by sildenafil with an IC_{50} value of 1.3 $\pm$ 0.9 μM (Figure 7B). PDE6 is most sensitive to sildenafil, with an IC_{50} value of 25 $\pm$ 5 nM (Figure 7B); for zaprinast, this value is 0.65 $\pm$ 0.15 μM (Figure 7A). Interestingly, previous work has shown that *Drosophila* tubule cG-PDE activity exhibits nanomolar sensitivity to sildenafil [13]. It is possible, then, that PDE6 may be the main *in vivo* target for this drug in tubules. Finally, PDE11 shows sensitivity to both zaprinast and sildenafil, with IC_{50} values of 1.6 $\pm$ 0.5 μM (Figure 7A) and 0.12 $\pm$ 0.06 μM (Figure 7B) respectively.

DISCUSSION

Previous work has shown that cG-PDE activity is important for regulating fluid transport by the *Drosophila* Malpighian tubule. However, surprisingly, *Drosophila* PDEs have not been well characterized to date, beyond the work on *dunce*. Given this, we investigated candidate PDEs using *D. melanogaster* genome resources. We show that *Drosophila* encodes several novel PDEs. By homology, these include two cG-PDEs (PDE6 and PDE9),

Table 3 Comparison of known *Drosophila* cG-PDEs with vertebrate cG-PDEs

Data from Figures 5–7 are tabulated to aid comparison with vertebrate homologues of *Drosophila* PDEs. Values for K_m (cGMP and cAMP) and IC_{50} values for zaprinast and sildenafil are listed, where known, with appropriate references. ND, not determined.

Enzyme	K_m cGMP (μM)	K_m cAMP (μM)	IC_{50} zaprinast (μM)	IC_{50} sildenafil (μM)
Drosophila PDE1	15.3 ± 1	20.5 ± 1.5	71 ± 39	1.3 ± 0.9
PDE1C	2.2 ± 0.1 (Mouse [43])	3.5 ± 0.3 (Mouse [43])	3.5 ± 0.6 (Human [44])	1.1 ± 0.275 (Bovine aorta *PDE1* [45])
Drosophila PDE6	37 ± 13	ND	0.65 ± 0.15	0.025 ± 0.005
PDE6β	17 ± 7 (Bovine [46])	ND	0.18 ± 0.01 {Human (K_i) [47]}	0.02 ± 0.001 (Human (K_i) [47])
Drosophila PDE11	6 ± 2	18.5 ± 5.5	1.6 ± 0.5	0.12 ± 0.06
PDE11A	0.52 ± 0.34 (Human PDE11A1 [48])	1.04 ± 0.23 (Human PDE11A1 [48])	12 (Human PDE11A1 [48])	3.8 ± 0.75 (Human PDE11A4 [49])

a cA-PDE (PDE8A) and two dual-specificity PDEs (PDE1 and PDE11). This, together with documented widespread expression of all PDE genes in the adult fly, suggests an important role for complex cyclic nucleotide regulation in the physiology of the fly.

Interestingly, the *Drosophila* genome does not encode homologues of mammalian PDE2, PDE3, PDE5, PDE7 and PDE10. This perhaps suggests that the *Drosophila* enzymes are products of ancestral genes, which in vertebrates evolved to encompass several other related PDEs that confer specialization of signalling processes in a necessarily more complicated body plan. For example, in *D. melanogaster*, PDE6 is the closest homologue of vertebrate PDE5. In mammals, PDE6 expression is confined to the eye and pineal gland, whereas in eye, it is an essential component of phototransduction [40]; recently, however, PDE6 expression has also been documented in Chinese hamster ovary and mouse F9 stem cells [41]. In the present study, we show that *D. melanogaster* PDE6 is widely expressed throughout the adult fly, suggesting multiple physiological roles for this PDE *in vivo*.

A striking observation from our work is the close similarity between the novel fly PDEs and their mammalian homologues. Not only is there a close sequence identity between the catalytic domains (59–77 %), but the regulatory and post-translational modification domains and motifs are also very similar. However, in common with many proteins encoded by the *Drosophila* genome, the *Drosophila* PDEs have long insertions at the N- and C-termini. Although the significance of these is unknown, it may suggest that further regulation may exist for *Drosophila* PDE function. Another example of this is demonstrated by comparing *Drosophila* PDE6 with mammalian retinal PDE6. Whilst all three mammalian retinal PDE6 catalytic subunits contain the CAAX-box prenylation motif, none has the proximal polybasic region contained in the *Drosophila* enzyme. Thus sequence information raises interesting questions regarding regulation, expression and post-translational modification of these novel PDEs.

We also present the first detailed biochemical analysis of novel *Drosophila* PDEs. The present study allows assignments of these *Drosophila* PDEs with their mammalian counterparts, based on biochemical function, in addition to sequence similarity. From these studies, we show that *D. melanogaster* PDE1 is a dual-specificity, Ca^{2+}/calmodulin-regulated enzyme. Thus, in spite of having structural differences from mammalian PDE1C, e.g. the *Drosophila* enzyme contains only one calmodulin-binding site and not two (Figure 2, and see Supplementary Figure 1 at http://www.BiochemJ.org/bj/388/bj3880333add.htm), this enzyme performs as *bona fide* PDE1.

PDE6 is the most sensitive enzyme to cGMP, although low cAMP-hydrolysing activity is detected in IP samples of this enzyme. However, given that PDE6 is the closet homologue of vertebrate PDE5 and that residues deemed critical to the PDE5 mode of action [20] are conserved within the PDE6 catalytic domain (Q935, Q893, A885 and W970, see Supplementary Figure 1 at http://www.BiochemJ.org/bj/388/bj3880333add.htm) allowed us to assign PDE6 as a cG-PDE.

PDE11 is a dual-specificity PDE, as is its vertebrate homologue. However, compared with PDE1 and PDE6, in *Drosophila*, PDE11 possesses the highest affinity for cGMP.

All of the novel *Drosophila* PDEs characterized in the present study display sensitivity to known inhibitors of vertebrate PDEs, i.e. zaprinast and sildenafil (Figure 6 and Table 3). This correlates well with previous studies that demonstrated sensitivity of cG-PDE activity and Malpighian (renal) tubule function to zaprinast [2] and sildenafil [13]. PDE6, in particular, displays nanomolar sensitivity to sildenafil, as well as submicromolar sensitivity to zaprinast.

Thus, taken together, the *Drosophila* PDEs have reassuring similarities but intriguing differences, at both the gene and protein level, compared with vertebrate PDEs. For example, although *dunce* and *PDE4* are close homologues, *dunce*-encoded PDE is not inhibited by the PDE4-specific inhibitor, rolipram [42]. Thus, given the value of PDEs as drug targets, our findings may allow rational drug design based on identified structure–function relationships between vertebrate and *Drosophila* enzymes and may also allow strategies for novel insecticide discovery.

Furthermore, following on from the characterization studies, analysis of PDE function *in vivo*, using transgenesis and mutagenesis in *Drosophila*, will allow discovery of fundamental physiological processes governed by cG-PDEs.

This work was supported by grants from the U.K. Biotechnology and Biological Sciences Research Council (to S.-A.D. and J.A.T.D.), the U.K. Medical Research Council (to M.D.H.) and a Wellcome Trust studentship (to J.P.D.). We are grateful to S. Francis (Vanderbilt School of Medicine, Nashville, TN, U.S.A.) for the gift of sildenafil citrate; to S. Francis, N.J. Pyne and K.E. Broderick for helpful discussion; and to M.R. MacPherson and A.C. Godfrey for help with experiments.

REFERENCES

1 Mullershausen, F., Friebe, A., Feil, R., Thompson, W. J., Hofmann, F. and Koesling, D. (2003) Direct activation of PDE5 by cGMP: long-term effects within NO/cGMP signaling. J. Cell Biol. **160**, 719–727

2 Broderick, K. E., MacPherson, M. R., Regulski, M., Tully, T., Dow, J. A. T. and Davies, S. A. (2003) Interactions between epithelial nitric oxide signaling and phosphodiesterase activity in Drosophila. Am. J. Physiol. Cell Physiol. **285**, C1207–C1218

3 Murthy, K. S. (2001) Activation of phosphodiesterase 5 and inhibition of guanylate cyclase by cGMP-dependent protein kinase in smooth muscle. Biochem. J. **360**, 199–208

4 Mehats, C., Andersen, C. B., Filopanti, M., Jin, S. L. and Conti, M. (2002) Cyclic nucleotide phosphodiesterases and their role in endocrine cell signaling. Trends Endocrinol. Metab. **13**, 29–35

5 Francis, S. H., Turko, I. V. and Corbin, J. D. (2001) Cyclic nucleotide phosphodiesterases: relating structure and function. Prog. Nucleic Acid Res. Mol. Biol. **65**, 1–52

6 Davis, R. L. and Dauwalder, B. (1991) The *Drosophila* dunce locus: learning and memory genes in the fly. Trends Genet. **7**, 224–229

7 Hansen, G., Jin, S., Umetsu, D. T. and Conti, M. (2000) Absence of muscarinic cholinergic airway responses in mice deficient in the cyclic nucleotide phosphodiesterase PDE4D. Proc. Natl. Acad. Sci. U.S.A. **97**, 6751–6756

8 Houslay, M. D. (2001) PDE4 cAMP-specific phosphodiesterases. Prog. Nucleic Acid Res. Mol. Biol. **69**, 249–315

9 Houslay, M. D. and Adams, D. R. (2003) PDE4 cAMP phosphodiesterases: modular enzymes that orchestrate signalling cross-talk, desensitization and compartmentalization. Biochem. J. **370**, 1–18

10 O'Donnell, J. M. and Zhang, H. T. (2004) Antidepressant effects of inhibitors of cAMP phosphodiesterase (PDE4). Trends Pharmacol. Sci. **25**, 158–163

11 Spina, D. (2004) The potential of PDE4 inhibitors in respiratory disease. Curr. Drug Targets Inflamm. Allergy **3**, 231–236

12 Brand, A. H. and Perrimon, N. (1993) Targetted gene expression as a means of altering cell fates and generating dominant phenotypes. Development **118**, 401–415

13 Broderick, K. E., Kean, L., Dow, J. A. T., Pyne, N. J. and Davies, S. A. (2004) Ectopic expression of bovine type 5 phosphodiesterase confers a renal phenotype in Drosophila. J. Biol. Chem. **279**, 8159–8168

14 Dow, J. A. T. and Davies, S. A. (2003) Integrative physiology, functional genomics and epithelial function in a genetic model organism. Physiol. Rev. **83**, 687–729

15 Dow, J. A. T., Maddrell, S. H., Davies, S. A., Skaer, N. J. and Kaiser, K. (1994) A novel role for the nitric oxide-cGMP signaling pathway: the control of epithelial function in Drosophila. Am. J. Physiol. **266**, R1716–R1719

16 Davies, S.-A. (2000) Nitric oxide signalling in insects. Insect. Biochem. Mol. Biol. **30**, 1123–1138

17 MacPherson, M. R., Broderick, K. E., Graham, S., Day, J. P., Houslay, M. D., Dow, J. A. and Davies, S. A. (2004) The dg2 (for) gene confers a renal phenotype in Drosophila by modulation of cGMP-specific phosphodiesterase. J. Exp. Biol. **207**, 2769–2776

18 MacPherson, M. R., Lohmann, S. M. and Davies, S. A. (2004) Analysis of Drosophila cGMP-dependent protein kinases and assessment of their *in vivo* roles by targetted expression in a renal transporting epithelium. J. Biol. Chem. **279**, 40026–40034

19 Torrie, L. S., Radford, J. C., Southall, T. D., Kean, L., Dinsmore, A. J., Davies, S. A. and Dow, J. A. (2004) Resolution of the insect ouabain paradox. Proc. Natl. Acad. Sci. U.S.A. **101**, 13689–13693

20 Zhang, K. Y., Card, G. L., Suzuki, Y., Artis, D. R., Fong, D., Gillette, S., Hsieh, D., Neiman, J., West, B. L., Zhang, C. et al. (2004) A glutamine switch mechanism for nucleotide selectivity by phosphodiesterases. Mol. Cell **15**, 279–286

21 Radford, J. C., Davies, S. A. and Dow, J. A. (2002) Systematic G-protein-coupled receptor analysis in Drosophila melanogaster identifies a leucokinin receptor with novel roles. J. Biol. Chem. **277**, 38810–38817

22 Bolger, G. B., McCahill, A., Huston, E., Cheung, Y. F., McSorley, T., Baillie, G. S. and Houslay, M. D. (2003) The unique amino-terminal region of the PDE4D5 cAMP phosphodiesterase isoform confers preferential interaction with beta-arrestins. J. Biol. Chem. **278**, 49230–49238

23 Charbonneau, H., Prusti, R. K., LeTrong, H., Sonnenburg, W. K., Mullaney, P. J., Walsh, K. A. and Beavo, J. A. (1990) Identification of a noncatalytic cGMP-binding domain conserved in both the cGMP-stimulated and photoreceptor cyclic nucleotide phosphodiesterases. Proc. Natl. Acad. Sci. U.S.A. **87**, 288–292

24 Walter, M. F. and Kiger, Jr, J. A. (1984) The Dunce gene of Drosophila: roles of Ca^{2+} and calmodulin in adenosine 3′:5′-cyclic monophosphate-specific phosphodiesterase activity. J. Neurosci. **4**, 495–501

25 Sonnenburg, W. K., Seger, D., Kwak, K. S., Huang, J., Charbonneau, H. and Beavo, J. A. (1995) Identification of inhibitory and calmodulin-binding domains of the PDE1A1 and PDE1A2 calmodulin-stimulated cyclic nucleotide phosphodiesterases. J. Biol. Chem. **270**, 30989–31000

26 Muradov, K. G., Boyd, K. K., Martinez, S. E., Beavo, J. A. and Artemyev, N. O. (2003) The GAFa domains of rod cGMP-phosphodiesterase 6 determine the selectivity of the enzyme dimerization. J. Biol. Chem. **278**, 10594–10601

27 Resh, M. D. (2004) Membrane targeting of lipid modified signal transduction proteins. Subcell. Biochem. **37**, 217–232

28 Wang, J. (2004) Nucleotide-dependent domain motions within rings of the RecA/AAA(+) superfamily. J. Struct. Biol. **148**, 259–267

29 Ponting, C. P. and Aravind, L. (1997) PAS: a multifunctional domain family comes to light. Curr. Biol. **7**, R674–R677

30 Hayashi, M., Matsushima, K., Ohashi, H., Tsunoda, H., Murase, S., Kawarada, Y. and Tanaka, T. (1998) Molecular cloning and characterization of human PDE8B, a novel thyroid-specific isozyme of 3′,5′-cyclic nucleotide phosphodiesterase. Biochem. Biophys. Res. Commun. **250**, 751–756

31 Soderling, S. H., Bayuga, S. J. and Beavo, J. A. (1998) Cloning and characterization of a cAMP-specific cyclic nucleotide phosphodiesterase. Proc. Natl. Acad. Sci. U.S.A. **95**, 8991–8996

32 Soderling, S. H., Bayuga, S. J. and Beavo, J. A. (1998) Identification and characterization of a novel family of cyclic nucleotide phosphodiesterases. J. Biol. Chem. **273**, 15553–15558

33 Corbin, J. D., Turko, I. V., Beasley, A. and Francis, S. H. (2000) Phosphorylation of phosphodiesterase-5 by cyclic nucleotide-dependent protein kinase alters its catalytic and allosteric cGMP-binding activities. Eur. J. Biochem. **267**, 2760–2767

34 Thomas, M. K., Francis, S. H. and Corbin, J. D. (1990) Substrate- and kinase-directed regulation of phosphorylation of a cGMP-binding phosphodiesterase by cGMP. J. Biol. Chem. **265**, 14971–14978

35 Wang, J., Kean, L., Yang, J., Allan, A. K., Davies, S. A., Herzyk, P. and Dow, J. A. (2004) Function-informed transcriptome analysis of Drosophila renal tubule. Genome Biol. **5**, R69

36 Day, J. P., Houslay, M. D. and Davies, S. A. (2003) Cloning and characterisation of a novel cGMP-specific phosphodiesterase from Drosophila melanogaster. BMC Meeting Abstracts: 1st International Conference on cGMP: NO/sGC Interaction and its Therapeutic Implications, 1:p0014

37 Fink, T. L., Francis, S. H., Beasley, A., Grimes, K. A. and Corbin, J. D. (1999) Expression of an active, monomeric catalytic domain of the cGMP-binding cGMP-specific phosphodiesterase (PDE5). J. Biol. Chem. **274**, 34613–34620

38 Xu, R. X., Hassell, A. M., Vanderwall, D., Lambert, M. H., Holmes, W. D., Luther, M. A., Rocque, W. J., Milburn, M. V., Zhao, Y., Ke, H. et al. (2000) Atomic structure of PDE4: insights into phosphodiesterase mechanism and specificity. Science **288**, 1822–1825

39 Xu, R. X., Rocque, W. J., Lambert, M. H., Vanderwall, D. E., Luther, M. A. and Nolte, R. T. (2004) Crystal structures of the catalytic domain of phosphodiesterase 4B complexed with AMP, 8-Br-AMP, and rolipram. J. Mol. Biol. **337**, 355–365

40 Yamazaki, A., Moskvin, O. and Yamazaki, R. K. (2002) Phosphorylation by cyclin-dependent protein kinase 5 of the regulatory subunit (Pgamma) of retinal cgmp phosphodiesterase (PDE6): its implications in phototransduction. Adv. Exp. Med. Biol. **514**, 131–153

41 Ahumada, A., Slusarski, D. C., Liu, X., Moon, R. T., Malbon, C. C. and Wang, H. Y. (2002) Signaling of rat frizzled-2 through phosphodiesterase and cyclic GMP. Science **298**, 2006–2010

42 Henkel-Tigges, J. and Davis, R. L. (1990) Rat homologs of the Drosophila dunce gene code for cyclic AMP phosphodiesterases sensitive to rolipram and RO 20-1724. Mol. Pharmacol. **37**, 7–10

43 Yan, C., Zhao, A. Z., Bentley, J. K. and Beavo, J. A. (1996) The calmodulin-dependent phosphodiesterase gene PDE1C encodes several functionally different splice variants in a tissue-specific manner. J. Biol. Chem. **271**, 25699–25706

44 Loughney, K., Martins, T. J., Harris, E. A., Sadhu, K., Hicks, J. B., Sonnenburg, W. K., Beavo, J. A. and Ferguson, K. (1996) Isolation and characterization of cDNAs corresponding to two human calcium, calmodulin-regulated, 3′,5′-cyclic nucleotide phosphodiesterases. J. Biol. Chem. **271**, 796–806

45 Daugan, A., Grondin, P., Ruault, C., Le Monnier de Gouville, A. C., Coste, H., Linget, J. M., Kirilovsky, J., Hyafil, F. and Labaudiniere, R. (2003) The discovery of tadalafil: a novel and highly selective PDE5 inhibitor. 2: 2,3,6,7,12,12a-hexahydropyrazino[1′,2′:1,6]pyrido[3,4-b]indole-1,4-dione analogues. J. Med. Chem. **46**, 4533–4542

46 Gillespie, P. G. and Beavo, J. A. (1988) Characterization of a bovine cone photoreceptor phosphodiesterase purified by cyclic GMP-sepharose chromatography. J. Biol. Chem. **263**, 8133–8141

47 Zhang, J., Kuvelkar, R., Wu, P., Egan, R. W., Billah, M. M. and Wang, P. (2004) Differential inhibitor sensitivity between human recombinant and native photoreceptor cGMP-phosphodiesterases (PDE6s). Biochem. Pharmacol. **68**, 867–873

48 Fawcett, L., Baxendale, R., Stacey, P., McGrouther, C., Harrow, I., Soderling, S., Hetman, J., Beavo, J. A. and Phillips, S. C. (2000) Molecular cloning and characterization of a distinct human phosphodiesterase gene family: PDE11A. Proc. Natl. Acad. Sci. U.S.A. **97**, 3702–3707

49 Weeks, J. L., Zoraghi, R., Beasley, A., Sekhar, K. R., Francis, S. H. and Corbin, J. D. (2004) High biochemical selectivity of tadalafil, sildenafil and vardenafil for human phosphodiesterase 5A1 (PDE5) over PDE11A4 suggests the absence of PDE11A4 cross-reaction in patients. Int. J. Impot. Res. **17**, 5–9

Received 7 January 2005/25 January 2005; accepted 27 January 2005
Published as BJ Immediate Publication 27 January 2005, DOI 10.1042/BJ20050057